Mechanism of the Emulsion–Precipitation Polymerization of Chlorotrifluoroethylene. 1. Kinetics of the Polymerization

David L. Murray

Dow Corning Corporation, 2200 West Salzburg Road, Auburn, Michigan 48611

Irja Piirma*

Institute of Polymer Science, University of Akron, Akron, Ohio 44325-3909

*Received January 21, 1993; Revised Manuscript Received June 14, 1993**

ABSTRACT: Emulsion polymerizations of chlorotrifluoroethylene (CTFE) were performed employing ammonium persulfate as initiator and ammonium perfluorooctanoate as surfactant. The polymerization showed a pseudo-zero-order dependence on monomer concentration throughout 80% of the reaction. Increasing the initiator concentration produced faster polymerization rates and larger particle number densities, while the rate of polymerization per particle decreased slightly. The increase in the number of latex particles with increasing initiator concentration provided additional sites for the polymerization to occur, causing a lower radical entry rate and a lowering of the per particle rate of polymerization. This phenomenon of the polymerization accounted for the observed high initiator concentration rate order dependence (0.8) and the constancy of molecular weight with initiator concentration. Increases in surfactant concentration also increased the polymerization rate by increasing the particle number density. However, the rate per particle decreased by a factor of 40 with surfactant concentration which was most likely due to a decrease in the number of free radicals per particle in the smaller volume latex particles. Molecular weights of the polymers (PCTFE) were independent of the radical concentration within the particles but varied inversely with polymerization temperature. Molecular weight is believed to be controlled either by chain transfer to monomer or by a highly temperature-dependent termination process for the occluded radicals. This study revealed that the presence of occluded radicals in the polymer matrix accounts for many of the unexpected observed experimental results. Isolation of the radicals, in the emulsion–precipitation polymerization of CTFE, occurs not only among latex particles but also within the particles themselves.

Introduction

Any complete model for a heterophase polymerization must be able to account for both the kinetics and particle formation (i.e., nucleation) aspects of the polymerization. In the past, much effort has been focused on the emulsion polymerization of styrene and many kinetic models for this system have been proposed. However, a truly general model that encompasses all monomer–surfactant combinations has not been developed. The reason for the failure of an all-descriptive model stems from the complexity of the heterophase system. There are always at least two phases in which the polymerization can occur. Therefore, the best approach to follow when using any monomer–surfactant combination is to determine the characteristics of the system by direct experimental observation.

Within the general class of heterophase polymerizations are systems in which the polymer is not soluble in its own monomer. These monomer–polymer systems are unique since the polymer precipitates immediately when the polymerization begins. Emulsion polymerizations involving such monomers are very complex since segregation occurs not only between the monomer and continuous phase but also between the polymer and the monomer. This creates a truly heterogeneous system. Included in this class of polymerizations are those that involve several fluorinated monomers. Fluorinated monomers (e.g., tetrafluoroethylene (TFE), chlorotrifluoroethylene (CTFE), 1,2-difluoroethylene) have received much attention due to the chemical inertness of their corresponding polymers. Commercially, these monomers are polymerized under what is classically called emulsion polymerization.[1] This method is chosen in order to dissipate the heat generated by their highly exothermic polymerizations. However, almost no details on their kinetics or particle formation mechanisms exist. The polymerizations of these fluorinated monomers are plagued with problems, and hence published results are limited. Safety hazards are one of the major concerns when polymerizing these monomers. Although the polymers are generally inert, their monomers tend to be highly reactive. Great care must be taken to minimize oxygen reaction with these monomers, and one must be vigilant about safety when working with them. The literature contains safety precautions for these monomers, especially tetrafluoroethylene, the most dangerous of the three.[2] Experimental problems stem from the gaseous nature of the monomers and the semicrystalline nature of their polymers. This crystalline nature causes the polymers to have very limited solubility, making it difficult to determine the colligative properties of their solutions.

In this work, a study of the mechanism of chlorotrifluoroethylene polymerization under emulsion polymerization conditions was undertaken. To completely model the CTFE polymerization system, the role of the precipitated polymer on the overall mechanism was considered. Kinetics of the CTFE bulk and solution polymerization have been reported in the past, but all fail to include the role of heterogeneity in the system.[3,4] Even the "so-called" bulk polymerization of CTFE results in a second phase, thus causing the polymerization steps to be segregated between the phases. Therefore, an adequate model for the polymerization which includes the effect of particle formation on the kinetics is still needed.

Experimental Section

A. Materials. Ammonium persulfate obtained from Aldrich Chemical Co. was employed as the initiator and was used as received. Ammonium perfluorooctanoate (FC143) was kindly provided by 3M Corp. and was recrystallized from a 5:2

* Abstract published in *Advance ACS Abstracts*, September 1, 1993.

0024-9297/93/2226-5577$04.00/0

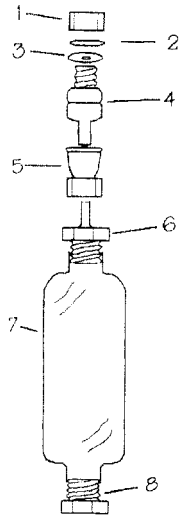

	Description	Swaglok Part #
1.	Compression Nut	
2.	Silicone Septa	
3.	Brass O-ring	
4.	Quick Connect Stem	(SS-QC4-D-200)
5.	Quick Connect Body	(SS-QC4-B-200)
6.	1/8" NPT-1/8" Pipe	(SS-TA-1-2)
7.	40 ml Sampling Cylinder	(304L-HDF2-40)
8.	Plug	(SS-2-P)

Figure 1. Schematic diagram of the reactor.

chloroform/acetone mixture. Chlorotrifluoroethylene (CTFE; bp −27 °C) was obtained from PCR Inc., noninhibited, and was flash-distilled from the cylinder before use. 2,5-Dichlorobenzotrifluoride was obtained from PCR Inc., 95% minimum purity, and was used as received. Nitrobenzene (D, 99%) was obtained from the Cambridge Isotope Laboratories refrigerated and used as received. The 1,3,5-trimethylbenzene (bp 162–164 °C) was obtained from Kodak Chemical Co. and was used as received. Water was deionized using a Corning MEGA-PURE deionization and filtration system equipped with a 0.2-μm filter. In all cases, the specific resistance of the water was greater than 14 MΩ cm^{-1}.

B. Polymerization Technique. Note: Care must be taken in the handling of CTFE. The presence of oxygen should be scrupulously avoided during the storage and transfer under pressure. The monomer may react with oxygen explosively with the formation of gaseous products and carbon. Small amounts of oxygen cause the formation of peroxides which, in turn, promote autopolymerization. Under no circumstances should the monomer be stored above 170 °F.

The polymerizations were carried out in 40-mL stainless steel reaction bombs. The bombs were constructed using plugged 40-mL stainless steel gas sampling cylinders to which was connected a double-shut-off quick-connect fitting as shown in Figure 1. Solutions of the surfactant and initiator in deionized water were prepared previous to the reaction. The same solution was used in each series of reactions in order to minimize error. The initiator solution was prepared fresh before each of the reactions. The reaction bombs were twice pressurized with nitrogen and evacuated to remove any traces of oxygen. This procedure was sufficient to eliminate inhibition of the reaction by oxygen. The deionized water, surfactant solution, and initiator solution were charged into the bomb via a silicone septum fitted into a male quick-connect valve. The bomb was weighed to assure the proper amount of each solution was charged. The bomb was placed into a dry ice/isopropyl alcohol bath, and CTFE was then flash-distilled into the bomb using the distillation setup shown in Figure 2. The approximate amount of CTFE distilled into the reactor was monitored using a thermocouple type flowmeter (Omega Industries) which was calibrated for CTFE. The weight of the reaction bomb was recorded to ensure that the proper amount of CTFE had been charged. The bomb was then placed in a clamp on the shaft of a preheated, thermostated water bath and rotated end-over-end at 45 rpm. The standard recipe and conditions used for the polymerizations in this study are given in Table I. The effect of each variable was then determined using the combinations of ingredients outlined in Table II.

The reactions were stopped at predetermined times by quickly placing the reactor bomb in an ice bath and venting the excess CTFE in the fume hood. The resulting latex was transferred into a sample vial, and a portion of the latex (ca. 1–2 g) was weighed into a preweighed aluminum dish. Methanol was added to coagulate the polymer. The pan was transferred to an oven at 70 °C to dry overnight and the percent conversion determined.

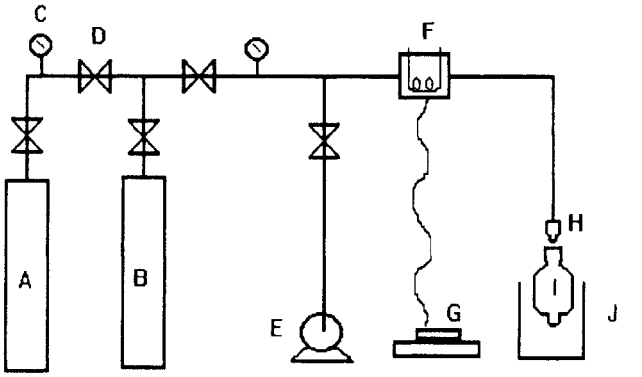

Figure 2. Setup for flash distillation of CTFE. A, CTFE cylinder; B, nitrogen cylinder; C, pressure gauge; D, valve; E, vacuum pump; F, TCD flowmeter; G, strip chart recorder; H, quick connect; I, reaction bomb; J, dry ice bath.

Table I. Standard Recipe Used in the Study

CTFE	20 g
deionized H_2O	100 g
$(NH_4)_2S_2O_8$	0.01 g
ammonium perfluorooctanoate	0.64 g
temperature	60 °C
rotation	45 rpm

Table II. List of Experimental Conditions used in the Study[a]

rxn no.	[S] × 10^3 (mol/L)	[I] × 10^3 (mol/L)	$[M]_0$ (mol/L)	temp (°C)	surfact type
1	14.80	10.00	1.72	60	FC-143
2	14.80	7.01	1.72	60	FC-143
3	14.80	4.75	1.72	60	FC-143
4	14.80	3.43	1.72	60	FC-143
5	14.80	2.38	1.72	60	FC-143
6	30.00	4.75	1.72	60	FC-143
7	22.30	4.75	1.72	60	FC-143
8	14.80	4.75	1.72	60	FC-143
9	9.74	4.75	1.72	60	FC-143
10	4.18	4.75	1.72	60	FC-143
11	14.80	4.75	2.40	60	FC-143
12	14.80	4.75	1.72	60	FC-143
13	14.80	4.75	1.03	60	FC-143
14	14.80	4.75	1.72	74	FC-143
15	14.80	4.75	1.72	60	FC-143
16	14.80	4.75	1.72	48	FC-143
17	14.80	4.75	1.72	40	FC-143
18	14.80	4.75	1.72	60	FC-143
19	14.80	4.75	1.72	60	SLS
20	14.80	4.75	1.72	60	$C_{10}F_{19}O_2NH_4$

[a] [S] = surfactant concentration, [I] = ammonium persulfate concentration, and $[M]_0$ = initial monomer concentration.

C. Rate of Polymerization. Plots of the percent conversion versus time were made using data obtained from several individual runs performed with constant reaction conditions. Attempts to derive conversion versus time curves from a single reaction failed due to the loss of CTFE gas during sampling. In all cases, at least five separate reactions were conducted for each recipe. The resulting plots yielded conversion versus time curves that were linear over a range of approximately 5–80% conversion. The slopes of the constant rate region were calculated using least-squares regression. The error in the least-squares fit was taken to be the error in the rate of polymerization. The rate of polymerization (R_p) was then determined using the following equation.

$$R_p = \frac{10(\text{slope})(W_m/W_w)d_w}{M_0} \quad (1)$$

In eq 1, R_p has units of mol L^{-1} s^{-1}, slope has units of % conv s^{-1}, W_m/W_w is the weight ratio of monomer to water, d_w is the density of water in g/cm^3, and M_0 is the molecular weight of the monomer.

D. Molecular Weight Measurements. Molecular weight distributions of poly(chlorotrifluoroethylene) (PCTFE) samples

were determined by high-performance size-exclusion chromatography (HPSEC) using a Waters 150C ALC/GPC which was equipped with refractive index and Viscotek Model 100 differential viscometer detectors. Two 6.2 mm × 25 cm silanized Du Pont Zorbax silica gel columns were coupled in series for the separation. The columns had a reported linear range of 1000–1 000 000 molecular weight based on polystyrene. The mobile phase was 2,5-dichlorobenzotrifluoride, and all runs were conducted with the entire system maintained at 130 °C. The injection volume was 250 μL.

The molecular weights were calculated based on the viscosity and refractive index detector data. The refractive index detector is a concentration-sensitive detector, while the viscosity detector is more sensitive to higher molecular weights. The intrinsic viscosity can be determined by combining the concentration data from the refractive index detector along with the viscosity data. The intrinsic viscosity is then the specific viscosity extrapolated to zero concentration. The molecular weight was related to the intrinsic viscosity, $[\eta]$, by the following equation.

$$[\eta] = KM^a = 6.15 \times 10^{-5} M^{0.74} \quad (2)$$

The K and a values for PCTFE were obtained from the literature for 2,5-dichlorobenzotrifluoride at 130 °C.[5] Integration and calculation of the molecular weight distribution were performed by the software supplied with the detectors.

E. Particle Sizing. 1. Transmission Electron Microscopy. A Jeol 120 transmission electron microscopy (TEM) was used to determine the particle sizes and particle size distributions of a few select samples of the PCTFE latices. The sample preparation for photographing in the TEM was performed as follows. Latices obtained from the experiments were diluted with deionized H_2O. A 100-mesh carbon-coated copper grid (Structure Probe Inc.) was placed onto an aluminum weighing dish. A Pasteur pipet was used to place a drop of the diluted latex onto the top of the grid. The grid was then covered and allowed to dry at room temperature overnight. A beaker of deionized water was heated to 60 °C, and the grids were washed by dipping the grid into the water and swirling it back and forth twice in order to remove the residual surfactant. The grids were then covered and allowed to dry overnight.

The grids were viewed under the TEM at a nominal magnification large enough to view several hundred particles. The actual magnification was determined by using a standard calibration grid which had 28 800 lines/in. A 3 × 5 in. negative was taken of the image in the TEM which was subsequently developed into an 8 × 10 in. print. The PCTFE particles on the print were counted and sized using a Carl Zeiss TGZ-3 particle size analyzer. Since some of the PCTFE particles are not round, an approximate diameter was measured that was in between the major and minor diameters of the egg-shaped particles. In addition, at least 750 particles were counted in order to minimize sampling error.

In some cases, the particles were shadowed in order to enhance the depth of field. This was accomplished by shadowing at an incident angle of 30° using a 60:40 gold/palladium alloy. A Jeol JEE 4C vacuum evaporator was employed for this process.

2. Dynamic Light Scattering (DLS). Several drops of the diluted latex sample (ca. 0.01 wt %) were placed into a square cuvette containing ca. 2.5 cm^3 of water. This cuvette was then placed into the sample compartment of a Malvern Autosizer IIc, a DLS instrument. The light scattering measurement was conducted at a fixed 90° angle. The scattered light signal was detected by a photomultiplier tube and analyzed by a K7032-NS computing correlator. A series of 10 measurements was performed on each sample. The information about the particle size and particle size distribution was computed by the software based on cumulant theory.

3. Particle Sizing Statistics. For calculation of the number of particles per cm^3 of the aqueous phase, N_p, the following equation was used:

$$N_p = \frac{(\%\ \text{conv})\left(\frac{W_w}{W_m}\right)(\rho_w)}{\left(\frac{\pi}{6}\right)(D \times 10^{-7})^3(\rho_p)} \quad (3)$$

where W_w/W_m is the monomer to water ratio in the polymerization recipe, ρ_w is the density of water, ρ_p is the density of the polymer, and D is the particle diameter in nanometers. The z-average diameter was used from the light scattering data, and the volume-average diameter was used from the TEM data.

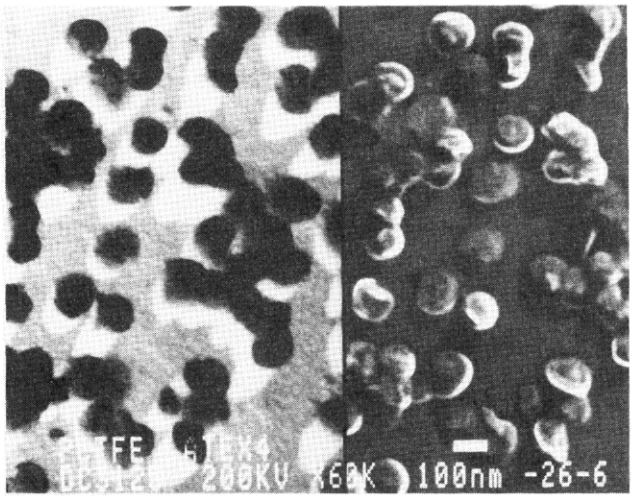

Figure 3. Shadowed SEM/TEM micrograph of the PCTFE particles at 95% conversion produced under the standard conditions shown in Table I.

F. ^{19}F Nuclear Magnetic Resonance. The ^{19}F-NMR spectra of the polymers were obtained to determine all different fluorine environments on the PCTFE chain. The spectra were obtained using a Varian XL 400 NMR spectrometer. Samples (5 wt %) of the polymer in a 80:20 w/w mixture of 1,3,5-trimethylbenzene and dueterated nitrobenzene (D, 99%) were prepared. In order to dissolve the samples, the temperature of the probe was maintained at 150 °C while the 376-MHz spectra were obtained. The spectral widths were all 50 kHz in order to look for all fluorine environments. Delay times of 2.0 s were used to allow for quantitative measurements. Chemical shifts reported are relative to hexafluorobenzene.

Results and Discussion

A. Results. The main goal of the kinetic study performed was to elucidate information on the polymerization mechanism. In order to formulate an adequate mechanism for the two-phase CTFE polymerization, the kinetic events occurring on the per particle scale were quantified since this reflects the radical entry and exit events for the particle. However, before this could be done, the change in the number density of the particles with conversion was determined.

Since PCTFE latex particles were not spherical, the selection of which technique (dynamic light scattering or transmission electron microscopy) to employ in measuring the average particle diameter was not straightforward. Figure 3 shows a micrograph of a typical latex produced under the standard recipe conditions listed in Table I. The particles in the photomicrograph have been shadowed at an incident angle of 30° to the grid in order to enhance the depth of field. At such angles, the length of the shadow should be ca. 2.5 times the radius of the particle. As can be seen in the micrograph, the shadow length is smaller than expected in many instances. Obviously, the particles are distorted in one dimension and can be characterized as flattened spheres.

Table III. Comparison of Particle Size Statistics from TEM and DLS

		TEM			
conv (%)	DLS: D_z (nm)	D_n (nm)	D_w (nm)	D_z (nm)	D_w/D_n
2	60	55	60	65	1.11
25	109	102	110	124	1.07
33	113	113	119	129	1.06
51	125	148	157	168	1.06
60	145	145	156	170	1.08
86	141	140	150	161	1.07
97	137	155	163	170	1.05

Table III shows the average particle diameters obtained from both TEM and DLS measurements. A quick scan of the data in Table III reveals that the z-average particle diameters obtained from DLS were smaller than the values obtained from TEM. In most other instances, the average diameters measured by DLS are larger than the values obtained by TEM. For polystyrene latices, this is due to swelling of the particles with monomer. In the case of CTFE, swelling of the polymer does not occur and the monomer evaporates immediately after the head pressure is removed from the reactor. This should cause the apparent particle size to be the same by both techniques. It may be that the nonspherical shape of the CTFE particles causes their size to appear larger in the TEM micrograph. This apparent larger particle diameter could stem from the fact that the particles on the TEM grid are laying on their flattened surfaces. This would cause the larger diameter of the particle to be exposed, and hence a larger diameter would be measured in the particle counter. In the DLS experiments, the diffusion coefficients of the particles are measured and the particle diameters are calculated assuming the particles are spherical. Since the particles appear to be smaller when measured by DLS, the particles' flattened shape seems to have a smaller influence on the diffusion coefficient than on their appearance in the TEM micrograph. Hence, it was believed that the results of the DLS experiment may reflect more accurately the true size of the latex, and the z-average diameter obtained from DLS was used in all calculations of the particle number density.

The change in the particle number density (N_p) with conversion at different initial surfactant concentrations was examined and is shown in Figure 4. The total number of particles increased with increasing surfactant concentration as expected, since there is more surfactant available to stabilize the smaller particles. The number of particles in the reaction increased abruptly in the first few percent conversion and then remained relatively constant in all cases. Scatter of the data in the higher concentration region arises from the use of data from individually prepared reactions. The error in determining the number of particles (using eq 3) involves both the error of the particle size measurement and the error in determining the conversion. The error in the percent conversion was estimated from the error in time and sample weight. The error in the particle size was calculated from repetitive DLS measurements of the same sample. This error is cubed in the particle number density calculations. Hence, the error in the particle number density was as large as 22% in some cases. Taking this error into account, the best estimate of the change in the particle number density (dN_p/dx) after 15% conversion is zero. After 15% conversion, it is most likely that either no new particles are nucleated or an equilibrium is established where the rate of new particle formation equals the rate of particle loss through coagulation. This is important since it allows for the per particle rate to be calculated during the constant

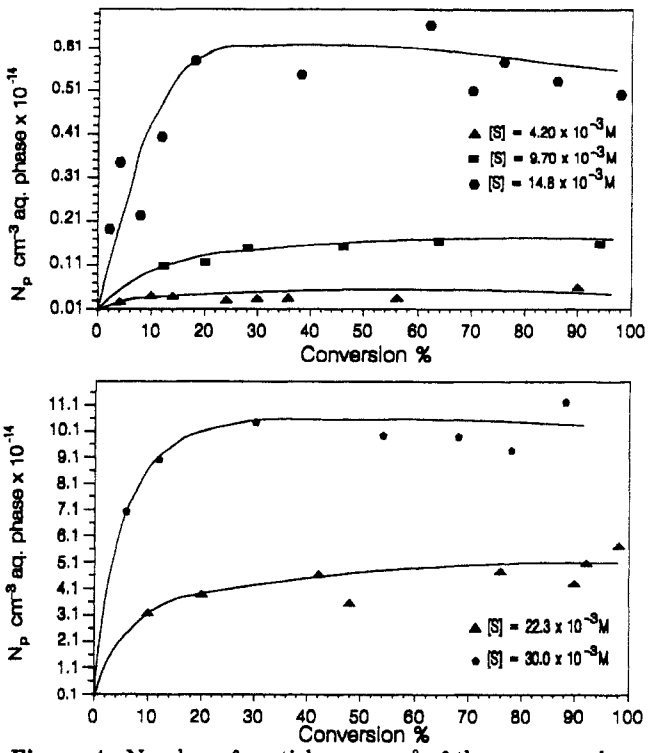

Figure 4. Number of particles per cm^3 of the aqueous phase versus conversion of different ammonium perfluorooctanoate levels. $[(NH_4)_2S_2O_8] = 4.75 \times 10^{-3}$ mol dm^{-3}, [CTFE] = 1.72 mol dm^{-3}, temp = 60 °C, 45 rpm.

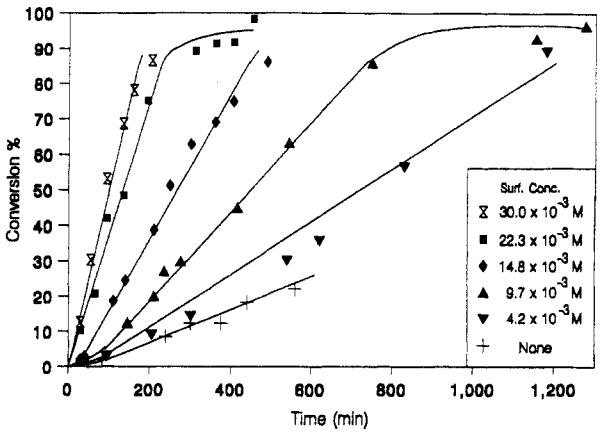

Figure 5. Conversion versus time plots for the polymerization of CTFE at different ammonium perfluorooctanoate concentrations. Temp = 60 °C, $[(NH_4)_2S_2O_8]$ 4.75 × 10^{-3} mol dm^{-3}, [CTFE] = 1.72 mol dm^{-3}, 45 rpm.

rate region. The rate per particle (R_p/N_t) was calculated by dividing the rate of polymerization for the constant rate region by the average total number of particles produced by each recipe.

1. **Reactant Concentrations.** The second step in the formulation of the polymerization mechanism was the establishment of the kinetic rate order dependencies for the reactant concentrations. Of general interest, the shapes of the conversion versus time plots for all the polymerizations were similar. Figure 5 demonstrates the general shape of these curves for the polymerization of CTFE at different surfactant concentrations. The sigmoidal conversion–time curve for these polymerizations is similar to those of typical emulsion polymerizations. A linear rate region, characteristic of the emulsion polymerization interval II, was always present. This constant rate region persisted from about 5 to 85% conversion, at which point the reaction rate slowed. This decreasing rate at the end of the polymerization is typical of the interval

Table IV. Molecular Weight of PCTFE with Conversion[a]

conv (%)	$[\eta]$ (dL/g)	$M_n \times 10^{-4}$	$M_w \times 10^{-5}$	M_w/M_n
24.6	0.31	7.9	1.39	1.9
33.0	0.28	7.3	1.51	1.9
60.5	0.27	6.9	1.31	1.9
98.5	0.32	7.9	1.82	2.3

[a] Temp = 60 °c, $[(NH_4)_2S_2O_8] = 4.75 \times 10^{-3}$ mol dm^{-3}, [S] = 1.48×10^{-2} mol dm^{-3}, 45 rpm, ammonium perfluorooctanoate.

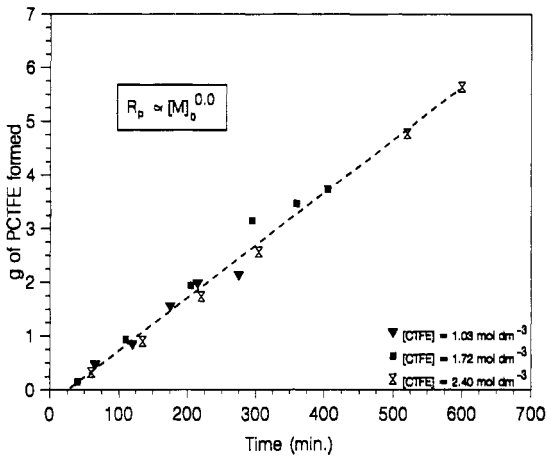

Figure 6. Initial monomer concentration effect on the rate of CTFE polymerization. Temp = 60 °C, $[(NH_4)_2S_2O_8] = 4.75 \times 10^{-3}$ mol dm^{-3}, [S] = 1.48×10^{-2} mol dm^{-3}, 45 rpm.

III region present in most emulsion polymerizations. Surprisingly, interval I, the typical increasing rate region at the beginning of the polymerization, was either unobserved or undetected due to insensitivity caused by the use of individually prepared polymerizations in the construction of the conversion–time plot.

No induction period was observed in these polymerizations, thus indicating that inhibition due to the presence of oxygen was not a factor and that the reaction preparation procedure sufficiently removed the oxygen. None of the conversion curves provided evidence of a gel effect since acceleration of the rate of polymerization was not observed during interval III. The molecular weight of the PCTFE produced at various degrees of conversion under the standard reaction conditions (Table I) was measured, and the results are listed in Table IV. The molecular weight was found to be constant with conversion and the polydispersity ratio was very close to that for a most probable distribution (2.0), indicating either a termination dominated by disproportionation or a first-order rate loss of radicals with time, such as in the case of a chain-transfer-dominated polymerization.

a. Initial Monomer Concentration. The linear region in the conversion versus time curve suggests that the polymerization was pseudo-zero-order in monomer concentration throughout 80% of the polymerization. The dependence of the rate of polymerization on the initial monomer concentration was also determined by plotting the grams of PCTFE formed with time at different initial monomer concentrations. The linearity of the plot, shown in Figure 6, demonstrates that the polymerization was also zero-order in initial monomer concentration.

b. Initiator Concentration. The dependence of the rate of polymerization on the ammonium persulfate concentration was determined by constructing a log–log plot of the rate of polymerization against the initiator concentration. The resulting plot, shown in Figure 7, reveals a rate order dependence of 0.8 in ammonium persulfate concentration at 60 °C. Figure 7 also displays the particle number density (N_p) dependence on the

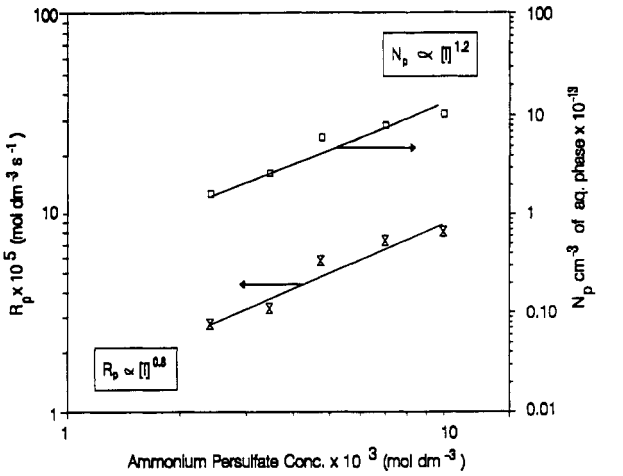

Figure 7. Dependence of the rate of polymerization and the particle number density on the concentration of ammonium persulfate. Temp = 60 °C, [CTFE] = 1.72 mol dm^{-3}, [S] = 1.48×10^{-2} mol dm^{-3}, 45 rpm.

Table V. Rate per Particle and the Particle Number Density Values for Polymerizations in Which the Initiator Concentration Was Varied[a]

[I] $\times 10^3$ (M)	R_p $\times 10^5$ (mol/L s)	D_z (nm)	N_p $\times 10^{-13}$ (cm^{-3}, aq)	R_p/N_t $\times 10^{20}$ (mol/L s)	$[\eta]$ (dL/g)	$M_n \times 10^{-4}$	M_w/M_n
2.38	2.72	155[b]	1.6	6.08	0.35	9.3	1.4
3.43	3.37	154[c]	2.6	5.18	0.30	8.3	2.5
4.75	6.13	136	6.1	4.03	0.23	7.9	2.3
7.01	7.33	125	8.0	3.66			
10.00	7.87	122	10.3	3.05	0.32	9.7	4.9

[a] Temperature = 60 °C, [S] = 1.48×10^{-2} mol dm^{-3}, 45 rpm, ammonium perfluorooctanoate. [b] 40% conversion. [c] 65% conversion.

concentration of ammonium persulfate. The increase in particle number density with increasing initiator concentration was followed by an increase in the polymerization rate. The dependence of N_p on the initiator concentration was found to be 1.2, which is quite large when compared to the emulsion polymerization of most monomers.

The per particle rate of polymerization was calculated and the molecular weight of the PCTFE at the end of the polymerization measured for the five different initiator concentrations. The results, listed in Table V, demonstrate that, as the concentration of ammonium persulfate is increased, the particle number density increases while the rate per particle decreases slightly and the molecular weight remains relatively constant.

2. Surfactant Concentration. Since the surfactant is not a reactant in the polymerization, its concentration can only exert influence on the polymerization by changing the particle number density. Figure 5 demonstrates the increase in polymerization rate with increasing surfactant concentration. The dependency of the particle number density and rate of polymerization on the surfactant concentration was calculated from the slope of the log–log plot shown in Figure 8. An increase in the polymerization rate follows an increase in the particle number density, demonstrating the importance of the number of reaction sites in increasing the overall rate of polymerization. Both the particle number density and the rate of polymerization dependence on surfactant concentration showed curvature in their log–log plots which indicates a rate order that is a function of the initial surfactant concentration. The rate order dependence on the ammonium perfluorooctanoate concentration was determined by fitting the data in Figure 9 to a second-order polynomial. The derivative of the fitted polynomial was determined and the rate order

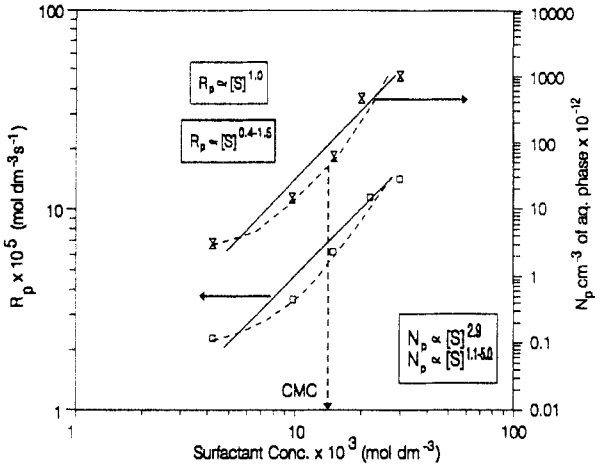

Figure 8. Rate of polymerization and particle number density dependence on the ammonium perfluoroctonate concentration. Temp = 60 °C, $[(NH_4)_2S_2O_8]$ = 4.75 × 10^{-3} mol dm^{-3}, [CTFE] = 1.72 mol dm^{-3}, 45 rpm.

Table VI. Rate per Particle and Particle Number Density Values for Polymerizations in Which the Surfactant Concentration Was Varied[a]

[S] × 10^3 (M)	R_p × 10^5 (mol/L s)	D_z (nm)	N_p × 10^{-13} (cm^{-3}, aq)	R_p/N_t × 10^{20} (mol/L s)	[η] (dL/g)	M_n × 10^{-4}	M_w/M_n
0.00	1.5						
4.18	2.3	302	0.4	23.9	0.21	5.3	3.8
9.74	3.5	215	1.5	9.7	0.23	6.0	2.3
14.8	6.1	136	6.1	4.0	0.23	6.1	2.3
22.3	11.4	68	45.7	1.0	0.25	6.4	3.0
30.0	14.1	53	99.6	0.6	0.30	8.2	2.3

[a] Temperature = 60 °C, [I] = 4.75 × 10^{-3} mol dm^{-3}, 45 rpm, ammonium perfluorooctanoate.

calculated for the high and low surfactant concentration regions. The results indicate a rate order dependence that increases from 0.4 at the low surfactant concentration to a value of 1.5 at the high surfactant concentration. The dependence of the particle number density on the ammonium perfluorooctanoate concentration was determined in the same manner. The particle number density dependence on the ammonium perfluorooctanoate concentration varies from 1.1 at the low surfactant concentration to a value of 5.0 at the high surfactant concentration.

The rate per particle was calculated for the different surfactant levels, and the results are displayed in Table VI. The rate per particle increases as the surfactant concentration decreases. The increase in the rate per particle is significant; it varies by a factor of 40 over the surfactant concentration range examined. However, despite the large variation in the rate per particle, the molecular weight of the polymer remains relatively constant.

3. Number of Particles. The change in surfactant concentration demonstrated the importance of the particle number density on the rate of polymerization. Thus, the dependency of the rate of polymerization on this variable was determined by plotting the log N_p versus log R_p as shown in Figure 9. Changes in N_p occurred for both initiator and surfactant concentration variations. However, the rate order dependence on the particle number density was not the same for these two reaction variables. Changes in N_p via surfactant concentration adjustments gave a rate order dependence of 0.33, while particle number density variations brought about by changes in initiator concentration gave a rate order dependence of 0.65. This indicates that the role of the particles depends on which

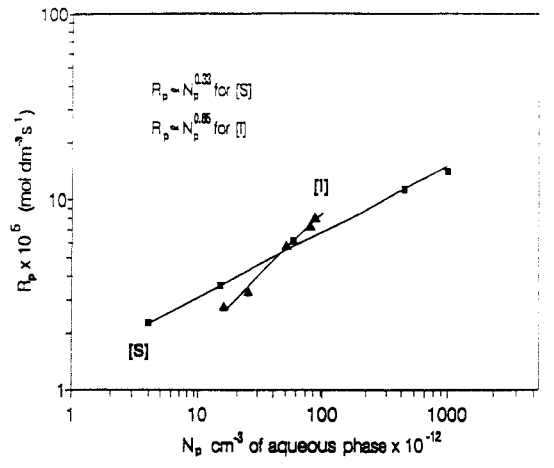

Figure 9. Effect of the particle number density on the rate of CTFE polymerization.

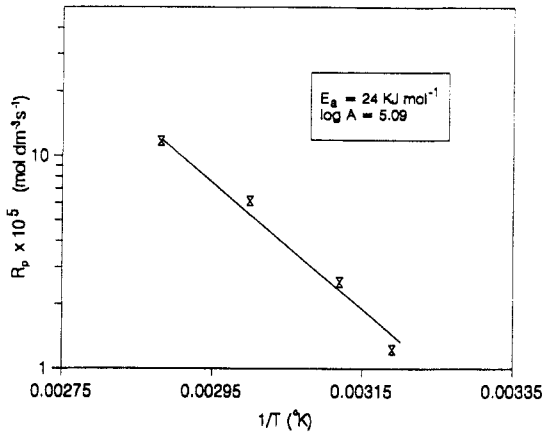

Figure 10. Arrhenius plot for the aqueous phase polymerization of CTFE. $[(NH_4)_2S_2O_8]$ = 4.75 × 10^{-3} mol dm^{-3}, [CTFE] = 1.72 mol dm^{-3}, [S] = 1.48 × 10^{-2} mol dm^{-3}, 45 rpm.

variables are changed. Both values are lower than predicted by Smith–Ewart case 2 kinetics,[6] which predicts a first-order dependence of the rate of polymerization on the number of particles. Therefore, Smith–Ewart case 2 kinetics does not hold and the average number of radicals per particle does not equal 0.5.

4. Temperature of Polymerization. The temperature of the polymerization was varied in order to determine the overall activation energy. However, along with the expected increase in the rate of polymerization with temperature, the particle number density also increased. The overall activation energy of the polymerization was calculated from the slope of the Arrhenius plot shown in Figure 10. A value of 24 kJ/mol was calculated, which was considerably lower than the value of 71 kJ/mol reported for the precipitation bulk polymerization of CTFE performed by Thomas and O'Shaughnessy.[3] The rate per particle was calculated and the molecular weight of the PCTFE at the end of the polymerization was measured for the various polymerization temperatures, and both are shown in Table VII. The rate per particle remained relatively constant with temperature, while the molecular weight was found to be inversely proportional to the polymerization temperature.

B. Discussion. The results of the kinetic study revealed some unconventional aspects of the polymerization of CTFE. First, the polymerization was observed to be pseudo-zero-order in monomer concentration both in this present investigation and in the bulk CTFE polymerization study performed by Thomas and O'Shaughnessy.[3] This pseudo-zero-order dependence in

Table VII. Rate per Particle and Particle Number Density Values for the Polymerizations in Which the Reaction Temperature Was Varied[a]

temp (°C)	R_p × 10^5 (mol/L s)	D_z (nm)	N_p × 10^{-13} (cm^{-3}, aq)	R_p/N_t × 10^{20} (mol/L s)	[η] (dL/g)	M_n × 10^{-4}	M_w/M_n
40	1.23	133[b]	3.9	1.25	0.65	21.5	2.2
48	2.55	124	3.8	2.68	0.47	15.7	4.1
60	6.13	136	6.1	4.03	0.23	7.9	2.3
74	11.7	105	15.5	3.02	0.19	5.0	15.0

[a] [I] = 4.75 × 10^{-3}, [S] = 1.48 × 10^{-2} M, 45 rpm, ammonium perfluorooctanoate. [b] 68% conversion.

the monomer concentration for both the studies indicates that the amount of monomer in the polymerization site was either constant or in large enough excess that the rate remained constant. The polymerization of CTFE in both of the investigations was devoid of any gel effect. Polymerizations conducted in high-viscosity environments, such as the PCTFE particle, would be expected to show a gel effect due to a reduced termination rate. Methyl methacrylate (MMA) is a monomer which has been shown to exhibit autoacceleration when polymerized in bulk. The absence of a gel effect in the emulsion polymerization of MMA was reasoned from the rate constant data of Ballard et al.,[7] who measured the propagation rate constant (k_p) for the polymerization as a function of conversion. The authors found that k_p actually decreased 2 orders of magnitude at high weight fractions of polymer. The decrease in the value of k_p for the polymerization was attributed to a change from a reaction energy barrier controlled propagation constant to a diffusion-controlled propagation constant. The decrease in k_p with conversion was large enough to compensate for the decrease in the rate of termination, thus avoiding acceleration of the polymerization. The same argument may apply to the emulsion polymerization of CTFE. The high-viscosity environment of the PCTFE particle could cause k_p to be diffusion-controlled throughout the entire polymerization. In other words, the diffusion of the monomer to the reaction site may be the rate-limiting step in the polymerization. This diffusion-controlled rate constant could be responsible for the absence of a gel effect in this polymerization and the pseudo-zero-order dependence on monomer concentration. In addition, a diffusion-controlled rate-determining step may explain the large differences in the recorded activation energies measured for the precipitation bulk and emulsion polymerization of CTFE. A diffusion-controlled rate would depend on how far the monomer must diffuse to reach the reaction site. The bulk precipitation polymerization of CTFE results in large agglomerates of polymer. Monomer may have to diffuse further into the polymer matrix in the bulk precipitation polymerization than it would for the small particles found in the emulsion polymerization of CTFE. This path-length difference would cause the overall rate of polymerization to appear lower in the bulk polymerization.

A second interesting feature of the CTFE emulsion polymerization was the 0.8 order dependence of the rate of polymerization on the initiator concentration. This value was observed both in this present work and in the work of Thomas and O'Shaughnessy.[3] The solution polymerization of CTFE in benzene and pentachloroethane also had reported rate order dependencies on initiator concentration of 0.7 and 0.8, respectively.[3,8] An important feature of all these polymerizations is the precipitation of the polymer immediately after the polymerization begins. Even the "so-called" solution and bulk polymerizations of CTFE are actually precipitation polymerizations in which particles are formed. The rate of polymerization per particle would prove to be a more useful way of looking at the kinetic events for these polymerizations. The rate of polymerization per particle is simply defined by eq 4.[9] In this equation, x is the

$$\frac{dx}{dt} = \frac{k_p N_p [M]_p \bar{n}}{n_m^0 N_A} \tag{4}$$

fractional conversion, N_p is the particle number density, k_p is the propagation rate constant, $[M]_p$ is the concentration of monomer in the particle, n_m^0 is the number of moles of monomer initially present, N_A is Avogadro's number, and $\bar{n}$ is the average number of free radicals in the particle. In regards to this study on the CTFE emulsion polymerization, eq 4 can be simplified by combining the constants. During the constant rate region, both the monomer concentration in the polymerization site and the number density of particles are constant. This reduces eq 4 to:

$$dx/dt = A\bar{n} \tag{5}$$

a collection of constants (A) multiplied by the average number of free radicals per particle. Thus, the rate per particle is an indication of the radical concentration within the particle and reflects its radical entry and exit events. The rate per particle was found to decrease with initiator concentration, although not as dramatically as with the surfactant concentration. On first thought this result would appear contrary to what one would expect. However, along with the change in the rate of polymerization was also a factor of 10 increase in the number of particles. If the number-average radical per particle is governed by $\bar{n} = \rho/(2\rho + k)$ (where k is the radical desorption rate coefficient), i.e., Smith–Ewart case I, then the strongest dependence of $\bar{n}$ on the radical entry rate (ρ) would be if $\bar{n} = \rho/k$ (i.e., $\bar{n}$ is very small).[9] Holding all other factors constant, then ρ would vary as N_p^{-1}, giving ρ = (function of [I])/N_p. Therefore, in this polymerization it appears that this function of [I] varies as $[I]^{0.8}$ which is quite normal especially if there is aqueous phase termination of the initiator-derived free radicals. This observation on the rate per particle was a significant finding which demonstrated that the increase in polymerization rate with increasing initiator concentration stems mostly from an overall increase in the number of propagating sites (i.e., the latex particles). Therefore, the expected effect of increased radical concentration, such as reduced molecular weights, was compensated for by the production of more particles which thereby slightly decrease the radical entry rate, and the effect of increasing the radical concentration by simply increasing the initiator concentration was not observed. A seeded run where the number of particles could be fixed for each experiment would need to be performed to observe this affect.

Particle number density variations brought about by ammonium perfluorooctanoate concentration changes had a different effect on the polymerization than the initiator concentration variations. The rate per particle was shown to decrease with the surfactant concentration and varied by a factor of 40 over the range examined in this study. This increase in the rate per particle could occur by an increase in the average number of free radicals per particle as demonstrated by eq 5. Apparently, as the particle number density decreases, the average number of free radicals per particle increases. A possible explanation as to how the number of free radicals per particle increases with decreasing surfactant concentration is as follows.

As the concentration of surfactant is decreased, the number of particles nucleated is also decreased. This gives fewer reaction sites for the initiator radicals to distribute themselves, causing an increase in the number of free radicals that enter a particular latex particle over time and as a result $\bar{n}$ increases (ρ is a function of $[N_p^{-1}]$). If termination of the radicals occurs once two radicals coexist in the same particle (i.e., the Smith–Ewart case 2 condition holds), the increase in the number of entering radicals would have little influence on the overall rate of polymerization and only the molecular weight of the polymer would decrease. In these CTFE polymerizations, the molecular weight of the PCTFE was independent of the rate per particle. This indicates that the polymer chains produced in the high-radical concentration particles can obtain the same degree of polymerization as the polymer chains in a low-radical concentration particle.

The best way to account for the increased free-radical concentration in the particle without a decrease in molecular weight is to assume suppression of the termination rate via radical occlusion. In this proposed mechanism, once a precipitating oligomeric radical coagulates with the particle it is free to polymerize with monomer diffusing into the particle. However, due to the high-viscosity environment in the PCTFE particle, the radicals on the chain ends are restricted from finding each other. As more radicals enter or coagulate with the particle, the overall number of free radicals increases and the rate per particle increases. However, total isolation of radicals in the polymer by matrix occlusion cannot be 100%. If the radicals within the particles were totally isolated from each other (i.e., the rate of termination was zero) then no affect of segregating the radicals among the particles by changing the particle number density would have been observed. The results indicate that changes in particle number density brought about by changes in the surfactant concentration do increase the overall rate. The efficiency of the particles in increasing the rate of polymerization was smaller for surfactant concentration changes ($R_p \propto N_p^{0.33}$) than for the particles produced when the initiator concentration was varied ($R_p \propto N_p^{0.65}$) which again points to the dependence of the radical entry rate on the initiator concentration.

If radical occlusion occurs, the rate per particle, and hence the number of radicals within a particle, was suspected to be a function of the volume. That is, the larger the volume of a particle, the more the likelihood of finding an occluded radical. To test this hypothesis, the rate per particle was plotted as a function of the cube of the z-average particle diameter. The value of the z-average particle diameter was chosen for each reaction between 90 and 100% conversion. The linearity of the plot, shown in Figure 11, demonstrates that the rate per particle is a linear function of particle volume. Occlusion of radicals in the emulsion precipitation polymerization of acrylonitrile was reported by McCarthy et al.[10] The average number of free radicals per particle during this aqueous-phase polymerization was calculated to be approximately 250. The paracrystalline nature of PACN is thought to be responsible for the occlusion of the radicals. PCTFE is also semicrystalline, and radicals have been shown to exist for long periods of time in the PCTFE matrix.[11] Hence, the idea of radical occlusion in this polymerization is well founded.

Two mechanisms for this polymerization exist in which the radicals can be isolated and thereby change the overall rate of the polymerization. First, radicals can be distributed among particles which are separated from each other

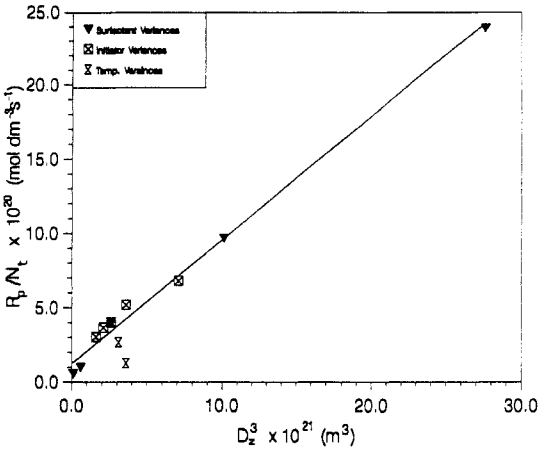

Figure 11. Dependence of the rate of polymerization per particle on the volume (D_z^3) of the particle near the end of the polymerization.

by the continuous phase. Second, the radicals can be isolated within the particle itself by occlusion in the crystalline polymer matrix. These two distinct mechanisms explain the difference in the rate order dependencies on particle number density calculated for the variant surfactant and initiator concentrations. Polymerization rate increases by isolation of radicals among the particles, dominated when the initiator concentration was changed. For surfactant concentration variations, radical occlusion in the PCTFE matrix helped keep the concentration of radicals high, hence increasing the rate per particle in the large particles produced at low surfactant concentrations.

A third interesting feature of the polymerization was the molecular weight variation with differing experimental conditions. The molecular weight was found to be independent of the initiator and surfactant concentrations (Tables V and VI). Even though the rate per particle varied by a factor of 40 over the surfactant concentration range, the molecular weight remained fairly constant (Table VI). The only reaction condition which changed the molecular weight was the temperature of polymerization. Lazar and Rado[12] also observed that molecular weight was only a function of temperature for the γ-irradiated solution polymerization of CTFE.

The typical expression employed to express the average chain length in a radical polymerization is the kinetic chain length (ν). This length is defined as the average number of monomer molecules polymerized per radical and is expressed mathematically as:

$$\nu = R_p/R_i \quad \text{or} \quad R_p/R_t \tag{6}$$

where R_p is the rate of polymerization, R_i is the rate of initiation, and R_t is the rate of termination. The rate of polymerization in a free-radical polymerization is given by the following:

$$R_p = k_p[M][M^*] \tag{7}$$

where k_p is the propagation rate constant, [M] is the concentration of monomer, and [M*] is the concentration of radicals. The termination process will depend on the square of the concentration of radicals as follows:

$$R_p = k_t[M^*]^2 \tag{8}$$

Substituting eq 7 and 8 into eq 6 demonstrates that, under steady-state radical concentrations, the kinetic chain length of the polymer should be inversely proportional to the radical concentration.

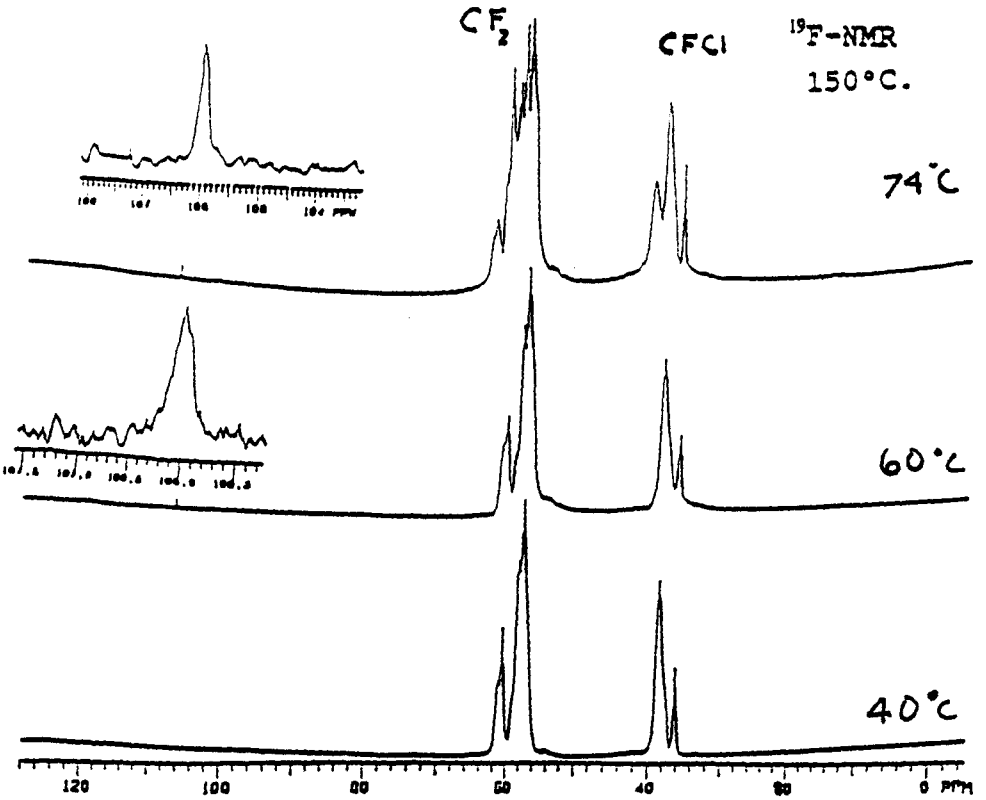

Figure 12. ^{19}F-NMR spectra of PCTFE samples polymerized at 40, 60, and 74 °C in a 80/20 wt % 1,3,5-trimethylbenzene/deuterated nitrobenzene mixture at 150 °C.

The inverse relationship of the radical concentration to the molecular weight did not hold in this polymerization. Changes in the rate per particle caused by varying the number of particles with surfactant concentration increased the average number of radicals per particle. This increase in radical concentration should have increased the rate of termination within the particle and decreased the molecular weight. Therefore, the results of this study were in contradiction to eq 10 and indicated that each radical within the particle was capable of adding the same number of monomer units.

Temperature changes, on the other hand, greatly influenced the molecular weight even though the rate per particle was constant (Table VII). Altering the polymerization temperature can affect many parameters of the polymerization. The solubility of CTFE in the aqueous phase is a function of temperature. Makitra et al.[13] measured the solubility of CTFE in water at 760 mmHg. The solubility of CTFE in water decreased from 4.69×10^{-5} mol dm^{-3} at 20 °C to 1.49×10^{-5} mol dm^{-3} at 60 °C. This fact would tend to predict a decrease in the rate of polymerization. Increased temperature may also activate a chain-transfer reaction, thereby decreasing the molecular weight. Chain transfer in this reaction would be limited to three species: the surfactant, the monomer, and the polymer. Chain transfer to the surfactant is unlikely due to its perfluorinated structure. Bryant[14] has calculated the thermodynamics of fluorine abstraction from polymer in the polymerization of tetrafluoroethylene (TFE). From these calculations, Bryant was able to rule out such abstractions from PTFE.

PCTFE samples polymerized at 40, 60, and 74 °C were examined using ^{19}F NMR. The spectra of these polymers are shown in Figure 12. Only two main fluorine environments are evident in the spectra at 36–40 and 56–62 ppm. These peaks correspond to the CFCl and CF_2 fluorine environments, respectively, and are consistent with the spectra reported by Cais and Kometani.[15] The splittings of the peaks was due to the stereosequencing of the polymer, and the pattern indicated a more atactic structure with increasing polymerization temperature. The pattern has been assigned and quantified by Cais and Kometani. The presence of only two different fluorine environments on the polymer chain eliminates the possibility of chain transfer to polymer. If chain transfer to polymer occurred, it would most likely involve the abstraction of a chlorine atom from the polymer chain. Chain transfer via a chlorine abstraction followed by propagation would leave a fluorine on a tertiary carbon. No tertiary fluorines were observed in the spectra. A small peak was observed at 106 ppm, but its intensity was in accordance with the chain end concentration. Chain transfer to polymer as a mode of molecular weight reduction does not seem to be a viable explanation.

The reduction in molecular weight appears to be associated with either chain transfer to monomer or an increased termination rate. The chain transfer to monomer, although chemically not intuitive, could explain much of the experimental phenomena. The ability of the CTFE polymerization to obtain 100% conversion when carried out in such a crystalline matrix would suggest a means by which the radicals can transfer out of the crystalline matrix such as in the case of vinyl chloride. Also, in systems in which chain transfer dominates and Smith–Ewart case 1 or 2 holds, the number-average molecular weight distribution (MWD) is given by:[9]

$$\exp\left(-\frac{C_M k_{tr} + [A]K_{tr,A} + \rho}{K_p C_M M_0}\right) \tag{9}$$

where M_0 is the molecular weight of monomer, A is the chain-transfer agent, C_M is the monomer concentration inside the particles, and ρ is the first-order rate coefficient for free-radical entry into the particle and is the instantaneous MWD. The actual MWD is the accumulation of these over a period of time. In the case where all chain

transfer to monomer occurs and $\rho \ll C_M K_{tr,M}$, then the cumulative number MWD reduces to:

$$\exp\left(-\frac{k_{tr,M}M}{k_p M_0}\right) \quad (10)$$

which is now independent of C_M. This suggestion implies that the MWD polydispersity will be close to 2, which is true of these polymerizations (Table VI), except for one run. This also suggests the temperature dependence of the number-average molecular weight to be given by k_u/k_p. If one assumes an activation energy difference between transfer and propagation of 5 kcal mol^{-1}, this would predict the M_n at 60 °C to be 0.6 times that at 40 °C, which is not a good approximation of the values observed experimentally in Table VII. However, the same argument could apply if the MWD was governed by k_t/k_p, such as temperature dependence for the occlusion of radicals and a 5 kcal mol^{-1} difference in these rate parameters.

Conclusions

The emulsion–precipitation polymerization of CTFE was found to be comparable to typical emulsion polymerizations in a few of its features. The shape of the conversion versus time curve showed a constant rate region throughout 80% of the polymerization. This indicated a monomer concentration in the polymerization loci that was constant, implying a monomer concentration that was diffusion-controlled. In addition, an increase in the particle number density increases the overall rate of polymerization. However, the rate of polymerization was not first-order in its particle number density dependence. Changes in the particle number density had different effects on the rate depending on whether or not other variables, such as the initiator concentration, were changed.

Many of the differences in the kinetic aspects of this polymerization emanate from the insolubility of the polymer in its monomer. This caused a segregation of the monomer from the polymer not common to most other emulsion polymerizations. The isolation of free radicals in this polymerization appears to occur by two different mechanisms. First, the particles in the polymerization were capable of isolating the radicals among themselves, as in most other emulsion polymerization systems. Therefore, increased particle number densities elevated the rate of polymerization by compartmentalizing the reaction among the particles. Second, the semicrystalline nature of the PCTFE was capable of isolating the radicals within a particle. Radical concentrations within the particle increased by a factor of 40 when the particle diameter was increased from 53 to 302 nm. The increase in the rate per particle was shown to be a linear function of the particle volume. The isolation of the radicals within a particle was not 100%, since an effect of the particle number density on the rate of polymerization was observed when the initiator concentration was held constant. Increases in the polymerization temperature were capable of causing an increase in a chain-stopping reaction. This was seen experimentally in a decrease of the molecular weight with polymerization temperature.

Acknowledgment. The authors thank Dow Corning Corp. for their support and funding which made this work possible.

References and Notes

(1) Putnam, R. In *Comprehensive Polymer Science*; Eastmond, et al., Eds.; Pergamon Press: New York, 1989; Vol. 3.
(2) Chandrasekaran, S. In *Encyclopedia of Polymer Science and Engineering*; Kroschwitz, J. I., Ed.; Wiley: New York, 1985; Vol. 3, p 463.
(3) Thomas, W. M.; O'Shaughnessy, M. T. *J. Polym. Sci.* **1953**, *11* (5), 455.
(4) Hamilton, J. R. *Ind. Eng. Chem.* **1953**, *45* (6), 1347.
(5) Walsh, E. K.; Kaufman, H. S. *J. Polym. Sci.* **1957**, *26*, 1.
(6) Smith, W.; Ewart, R. *J. Chem. Phys.* **1948**, *16*, 592.
(7) Ballard, M. J.; Napper, D. H.; Gilbert, R. G. *J. Polym. Sci., Polym. Chem. Ed.* **1984**, *22*, 3225.
(8) Lazar, M. *J. Polym. Sci.* **1958**, *14*, 573.
(9) Napper, D. H.; Gilbert, R. G. In *Comprehensive Polymer Science*; Eastmond, G. C., Ledwith, A., Russo, S., Sigwalt, P., Eds.; Pergamon Press: New York, 1989; Vol. 4, p 171.
(10) McCarthy, S. J.; Ebling, E. E.; Wilson, I. R.; Gilbert, R. G.; Napper, D. H.; Sangster, D. F. *Macromolecules* **1986**, *19*, 2440.
(11) Zehn, Xiang, *Radiat. Phys. Chem.* **1990**, *35*, 194.
(12) Lazar, M.; Rado, P. *Chem. Zvesti* **1956**, *10*, 120.
(13) Makitra, R. G.; Politanskaya, T. I.; Moin, F. B.; Kostyk, G. P. *Deposited Doc. VINITI* **1982**, 1.
(14) Bryant, W. M. D. *J. Polym. Sci.* **1962**, *56*, 277.
(15) Cais, R. E.; Kometani, J. M. *Macromolecules* **1984**, *17*, 1932.